Proceedings of the
Annual Stability Conference
Structural Stability Research Council
St. Louis, Missouri, April 2-5, 2019

Analytical and numerical buckling analysis of rectangular functionally-graded plates under uniaxial compression

Elias Y. Ali[1], Yared S. Bayleyegn[2]

Abstract

This paper presents analytical and numerical buckling analysis of a functionally-graded plate under uniaxial compression. Functionally graded materials (FGMs) are advanced composite materials which are characterized by gradual change in material properties within a given direction. The mechanical properties of the plate are assumed to vary continuously in the thickness direction using power law, sigmoid and exponential functions in terms of the volume fraction of constituent materials (metal and ceramic). Analytical and theoretical formulation for FGM plate buckling is conducted based on a first-order-shear deformation theory (FSDT) and the Galerkin method, an effective method for solving differential equations, was selected to solve an eigenvalue problem for determining the stability of FGM plate. Numerical analysis was then completed using ABAQUS to verify and validate the mathematical formulation. Parametric studies are then performed for different material models, aspect ratios, length to thickness ratios and plate boundary conditions. Finally, the optimum material gradation of the FGM plates was selected from numerical simulations. The results of this investigation demonstrate the potential application of FGMs as thin-walled structural component in the future development of resilient and sustainable structural components/systems.

1. Introduction

With increasing development in technology, manufacturing and construction process, the biggest challenge the material science and civil engineering community faces these days is selection of appropriate materials and the study of their responses under different loading environment. One of a new class of composite materials recently developed is functionally graded materials (FGMs). These are a new class of advanced materials characterized by non-homogenous material system with gradual gradation of material properties within a given dimension. This gradation is achieved by either combining two or more materials using volume-fraction or by treating a single material chemically to change its initial properties. The functionally graded composite material with then have a unique and different material properties from the individual constituent materials while preserving their individual benefits. Unlike the traditional composites, in which a reinforcing material is distributed throughout the bulk matrix material, FGMs are advanced composite in which two or more materials are mixed with a graded interface to avoid a distinct boundary between the bulk materials.

[1] PhD Candidate, Drexel University, <eya24@drexel.edu>
[2] Assistant Professor, Drexel University, <yaredshi@drexel.edu>

The history of man experimenting and combining two materials to get a better material is dated back to 2500 BC, when ancient humans learned to melt metals such as copper and tin from ore and began alloying the two metals to form bronze, which was much harder than its ingredients. Since then, for sole reason of improving material properties to modern day, man has been able to produce new class of material called composites. The original idea of compositional and material gradient for polymer materials was first proposed by Bever (1972) in 1972. The concept of FGM for engineering application was then first originated in Japan in 1984 during hypersonic space plane project as a thermal barrier to resist high temperature gradient (with outside temperature of 2000K and inside temperature of 1000K across 10 mm or less thickness) for space shuttles (Karam Y. Maalawi 2011, Rasheedat M. Mahamood 2012). That is, the body of the plane needs a composite material that would be exposed to a temperature gradient of 1000K, between the inside and outside of space plane. Conventional laminated composite was tried for this application, but they failed. The failure mode was due to delamination, that is the separation of the laminate composite materials from where the two materials were joined together. The researchers at the time understood that if the sharp interface between the two materials that forms the composite material could be eliminated, then the problem would be solved. Thus, they changed the sharp interface to gradient interface-by gradually introducing the second material to the first. Thus, using this method they were able to produce a new advanced material that was able to withstand the intended high temperature application. Numerous information about FGM are available in (Y. Miyamoto et al. 1999, Najafizadeh and Eslami 2002, Kieback et al. 2003, Birman and Byrd 2007, Bohidar et al. 2014, Bhavar et al. 2017).

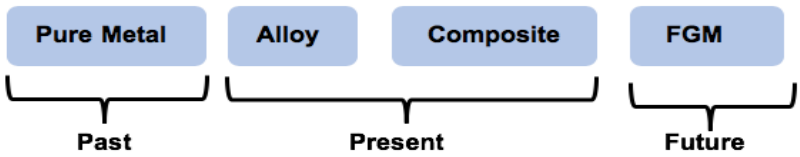

Figure 1: Development in engineering materials

The stability of rectangular functionally graded plates has been studied by several researchers in recent years. Reddy (2000) developed a finite element formulation theory for thermo-mechanical response of FGM using the higher-order shear deformation theory. Local buckling of rectangular FGM-stiffened plates based on classical plate theory was studied in Abdolvahab (2016). Stability and bifurcation analysis of a simply-supported FGM rectangular plate subject to transversal and in-plane excitations was studied by Sahari et al. (2016). Bodaghi and Saidi (2010) developed an exact analytical solution for buckling of functionally graded rectangular plates subjected to non-uniformly distributed in-plane loading acting on two opposite simply supported edges resting on elastic foundation. Ferreira et al. (2005) explores and analyze static deformations of a simply supported functionally graded plate modeled by a third-order shear deformation theory. Shariat et al. (2005) studied the buckling behavior of rectangular functionally graded plates with geometrical imperfections using equilibrium, stability, and compatibility equations using the classical plate theory for an imperfect functionally graded plate. Qian et al. (2004) studies the static deformations and free and forced vibrations of a thick rectangular functionally graded elastic plate by using a higher-order shear and normal deformable plate theory (HOSNDPT) and a meshless local Petrov–Galerkin (MLPG) method. Using the FSDT and finite element method, Anil Gite (2015) explores the buckling behavior of functionally graded plates under in-plane compression considering effect of geometrical parameters (i.e., aspect ratio, and slenderness ratio) on the mechanical buckling of FGM plate.

In this paper a mathematical formulation for FGM plate under uniaxial compression is derived using FSDT and the results are compared with available literature and with numerical simulation using FE package ABAQUS. The deformation and stress in the FGM plate are derived based on the assumptions provided in Chi and Chung (2006). Line elements perpendicular to the middle surface of the plate before deformation remain normal and un-stretched after deformation; the deflection of the FGM plate is small in comparison with its thickness h, such that the linear strain displacement relations are valid; the normal stress in the thickness direction can be neglected because the thickness which is assumed in the range 1/20 ~ 1/100 of its span is small and for the non-homogeneous elastic FGM plate, the Young's modulus and Poisson's ratio of the FGM plate are functions of the spatial coordinate (thickness).

2. Mechanical properties of FGM plate

FGMs are a mixture of ceramic and metal or a combination of different metals made by gradually varying the volume fraction of the constituent materials. The functionally graded material can be continually produced by varying the constituent multi-phase materials in a predetermined profile. The constitutive material property which varies with a given direction is expressed using volume fraction variation. This volume fraction variation can be described using power law function, sigmoid function or exponential function.

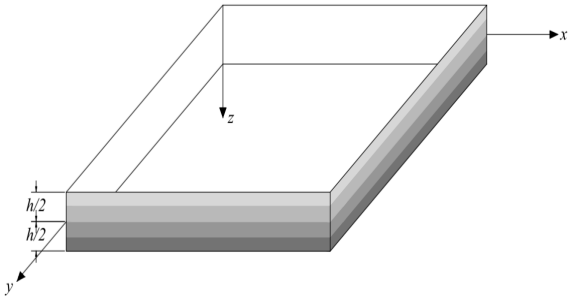

Figure 2: Material properties variation across the plate thickness

2.1 Power-law material function (P-FGM)

The volume fraction variation of FGM in power law function can be expressed with Eqn.1 along the thickness direction.

$$f(z)=\left(\frac{z+h/2}{h}\right)^{n} \tag{1}$$

Once the local volume fraction is defined, the functional relation of material properties at any point across the thickness of the plate can be expressed according to the general rule of mixtures. The young's modulus variation for P-FGM can be calculated Eq. 2

$$E(z)=f(z)E_2+\left[1-f(z)\right]E_1 \tag{2}$$

Where E_1 and E_2 are the Young's moduli of the FGM plate at bottom ($h/2$) and top ($-h/2$) surfaces. The variation of $E(z)$ in the plate thickness direction for P-FGM model is shown in Fig. 3.

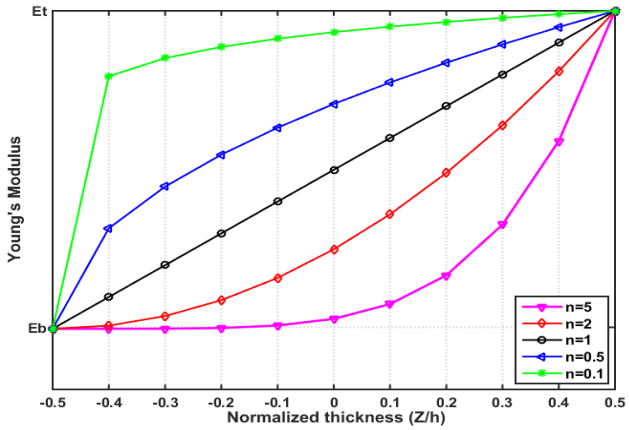

Figure 3: Variation of Young's modulus for P-FGM plate

2.2 Sigmoid material function (S-FGM)

The volume fraction variation of FGM in sigmoid function can be expressed with Eqns. (3- 4) along the thickness direction which is divided in to two parts of the FGM thickness.

$$f_1(z) = 1 - \frac{1}{2}\left(\frac{\frac{h}{2} - z}{\frac{h}{2}}\right)^P \quad for\ 0 \le z \le \frac{h}{2} \tag{3}$$

$$f_2(z) = \frac{1}{2}\left(\frac{\frac{h}{2} + z}{\frac{h}{2}}\right)^P \quad for -\frac{h}{2} \le z \le 0 \tag{4}$$

By using the rule of mixture, the Young's modulus of the S-FGM can be calculated by:

$$E(z) = f_1(z)E_1 + \left[1 - f_1(z)\right]E_2 \quad for\ 0 \le z \le \frac{h}{2} \tag{5}$$

$$E(z) = f_2(z)E_1 + \left[1 - f_2(z)\right]E_2 \quad for -\frac{h}{2} \le z \le 0 \tag{6}$$

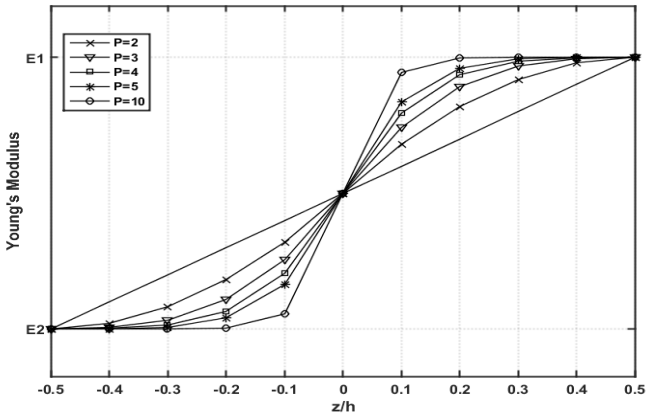

Figure 4: Variation of Young's modulus for S-FGM plate

2.3 Exponential material function (E-FGM)

The exponential function is used by many researchers to describe the variation of elastic modulus with the following function

$$E(z) = Ae^{B\left(z+\frac{h}{2}\right)} \tag{7}$$

Where $A = E_2$ and $B = \left(\frac{1}{h}\right)\ln\left(\frac{E_1}{E_2}\right)$

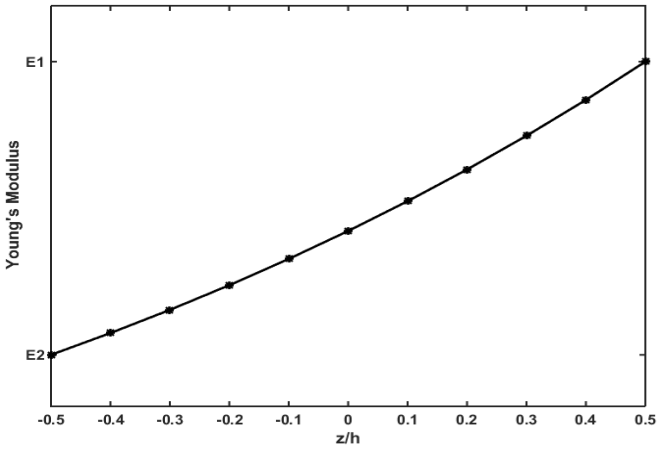

Figure 5: Variation of Young's modulus for E-FGM plate

3. Mathematical formulation of FGM plate

Based on the first assumption stated in (Chi and Chung 2006) , the transverse strain components are negligibly small. Therefore, the displacement at any point in the *x, y* and *z* direction can be expressed as:

$$u(x,y,z) = u_0(x,y) + z\frac{\partial w}{\partial x} \tag{8}$$

$$v(x,y,z) = v_0(x,y) + z\frac{\partial w}{\partial y} \tag{9}$$

$$w(x,y,z) = w_0(x,y) \tag{10}$$

Where

$$\begin{Bmatrix} \varepsilon_{xx} \\ \varepsilon_{yy} \\ \gamma_{xy} \end{Bmatrix} = \begin{Bmatrix} \varepsilon_{xx}^{\,0} \\ \varepsilon_{yy}^{\,0} \\ \gamma_{xy}^{\,0} \end{Bmatrix} + z\begin{Bmatrix} \varepsilon_{xx}^{\,1} \\ \varepsilon_{yy}^{\,1} \\ \gamma_{xy}^{\,1} \end{Bmatrix} \tag{11}$$

$$\begin{Bmatrix} \varepsilon_{xx}^{\,0} \\ \varepsilon_{yy}^{\,0} \\ \gamma_{xy}^{\,0} \end{Bmatrix} = \begin{Bmatrix} \frac{\partial u_0}{\partial x} \\ \frac{\partial v_0}{\partial y} \\ \frac{\partial u_0}{\partial y} + \frac{\partial v_0}{\partial x} \end{Bmatrix} \tag{12}$$

$$\begin{Bmatrix} \varepsilon_{xx}^{\ 1} \\ \varepsilon_{yy}^{\ 1} \\ \gamma_{xy}^{\ 1} \end{Bmatrix} = \begin{Bmatrix} \dfrac{\partial \phi_x}{\partial x} \\ \dfrac{\partial \phi_y}{\partial y} \\ \dfrac{\partial \phi_x}{\partial y} + \dfrac{\partial \phi_y}{\partial x} \end{Bmatrix} \tag{13}$$

3.1 Constitutive stress–strain relation of FGM plate

Based on the last two assumptions, the constitutive stress–strain relation for plane stress for an FGM plate can be expressed as:

$$\sigma_{xx} = \frac{E(z)}{1-\upsilon^2}\left\{ \varepsilon_{xx}^{\ 0} + v\varepsilon_{yy}^{\ 0} + z\left[\frac{\partial \phi_x}{\partial x} + v\frac{\partial \phi_y}{\partial y} \right] \right\} \tag{14}$$

$$\sigma_{yy} = \frac{E(z)}{1-\upsilon^2}\left\{ \varepsilon_{yy}^{\ 0} + v\varepsilon_{xx}^{\ 0} + z\left[\frac{\partial \phi_y}{\partial y} + v\frac{\partial \phi_x}{\partial x} \right] \right\} \tag{15}$$

$$\tau_{xy} = \frac{E(z)}{1-\upsilon^2}\left(\frac{1-v}{2} \right)\left[\gamma_{xy}^{\ 0} + 2\left(\frac{\partial \phi_x}{\partial y} + \frac{\partial \phi_y}{\partial x} \right) \right] \tag{16}$$

3.2 The axial forces, shear forces and the bending moment of FGM plate

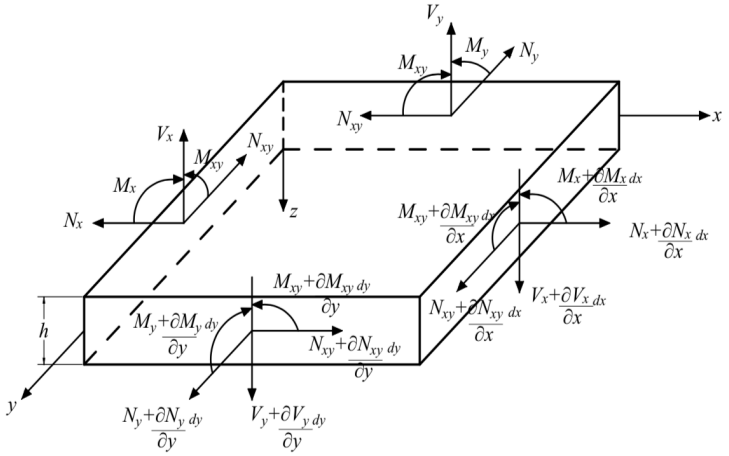

Figure 6: Forces in small solid FGM element

The stress resultants per unit length of the middle surface are defined by integrating stresses along the thickness and substituting the stress-strain relation in to stress resultants, the axial and bending moments can be expressed into matrix form as follows:

$$\begin{Bmatrix} N_x \\ N_y \\ N_{xy} \\ M_x \\ M_y \\ M_{xy} \end{Bmatrix} = \begin{bmatrix} A_{11} & A_{12} & 0 & B_{11} & B_{12} & 0 \\ A_{12} & A_{22} & 0 & B_{12} & B_{22} & 0 \\ 0 & 0 & A_{33} & 0 & 0 & B_{33} \\ B_{11} & B_{12} & 0 & C_{11} & C_{12} & 0 \\ B_{12} & B_{22} & 0 & C_{12} & C_{22} & 0 \\ 0 & 0 & B_{33} & 0 & 0 & C_{33} \end{bmatrix} \begin{Bmatrix} {\varepsilon_{xx}}^0 \\ {\varepsilon_{yy}}^0 \\ {\gamma_{xy}}^0 \\ \dfrac{\partial \phi_x}{\partial x} \\ \dfrac{\partial \phi_y}{\partial y} \\ 2\left(\dfrac{\partial \phi_x}{\partial y} + \dfrac{\partial \phi_y}{\partial x}\right) \end{Bmatrix} \tag{17}$$

Where the coefficients A_{ij}, B_{ij} and C_{ij} are the integration of the material properties of the FGM plate along the thickness and they are expressed as:

$$A_{11} = A_{22} = \int_{-h/2}^{h/2} \frac{E(z)}{1-\upsilon^2} dz,\ A_{12} = \int_{-h/2}^{h/2} \upsilon \frac{E(z)}{1-\upsilon^2} dz,\ A_{33} = \int_{-h/2}^{h/2} \frac{E(z)}{2(1-\upsilon)} dz$$

$$B_{11} = B_{22} = \int_{-h/2}^{h/2} z \frac{E(z)}{1-\upsilon^2} dz,\ B_{12} = \int_{-h/2}^{h/2} \upsilon z \frac{E(z)}{1-\upsilon^2} dz,\ B_{33} = \int_{-h/2}^{h/2} z \frac{E(z)}{2(1-\upsilon)} dz$$

$$C_{11} = C_{22} = \int_{-h/2}^{h/2} z^2 \frac{E(z)}{1-\upsilon^2} dz,\ C_{12} = \int_{-h/2}^{h/2} \upsilon z^2 \frac{E(z)}{1-\upsilon^2} dz, \quad C_{33} = \int_{-h/2}^{h/2} z^2 \frac{E(z)}{2(1-\upsilon)} dz \tag{18}$$

Flexural rigidity of FGM plate with constant poison ratio and varying Young's' modulus can be obtained from the coefficients with the following equation (Chi and Chung 2006)

$$\tilde{D} = B_{11}\left(\frac{-B_{11}}{A_{11}}\right) + C_{11} \tag{19}$$

3.3 Flexural rigidity solution for P-FGM plates

For P-FGM, substituting Eq. (2) into Eqn. (18), with MATLAB aid, one can obtain simplified solution for coefficients A_{ij}, B_{ij} and C_{ij} as shown below

$$A_{11} = A_{22} = \frac{h}{1-\upsilon^2}\left(\frac{nE_m + E_c}{n+1}\right) \tag{20a}$$

$$B_{11} = B_{22} = \frac{nh^2}{2(1-\upsilon^2)}\left(\frac{E_c - E_m}{(n+1)(n+2)}\right) \tag{20b}$$

$$C_{11} = C_{22} = \frac{h^3}{12(1-\upsilon^2)}\left[-E_m + 3(E_c - E_m)\frac{n^2+n+2}{(n+1)(n+2)(n+3)}\right] \tag{20c}$$

Flexural rigidity of FGM plate for P-FGM model with metal/ceramic materials can be evaluated using Eq. 19 and simplifying it will have the form

$$\tilde{\mathrm{D}} = \frac{I_1 I_3 - I_2^{\,2}}{I_1\left(1-\upsilon^2\right)} \tag{21}$$

Where:

$$I_1 = E_m h + \left(E_c - E_m\right)\frac{h}{n+1} \tag{22a}$$

$$I_2 = \left(E_c - E_m\right)h^2\left(\frac{1}{n+2} - \frac{1}{2n+2}\right) \tag{22b}$$

$$I_3 = E_m\frac{h^3}{12} + \left(E_c - E_m\right)h^3\left(\frac{1}{n+3} - \frac{1}{n+2} + \frac{1}{4n+4}\right) \tag{22c}$$

For a uniformly graded (Isotropic and homogenous) plate, E_c-E_m=0, such that Eqn. (21) can be reduced to well-known flexural rigidity for plate as

$$\mathrm{D} = \frac{Eh^3}{12\left(1-\upsilon^2\right)} \tag{23}$$

3.4 Flexural rigidity solution for S-FGM plates

With the steps like P-FGM plates, the coefficients A_{ij}, B_{ij} and C_{ij} for S-FGM plates can be expressed as

$$A_{11} = \frac{h}{1-\upsilon^2}\left(\frac{E_c - E_m}{2}\right) \tag{24a}$$

$$B_{11} = \frac{h^2}{8(1-\upsilon^2)}(E_c - E_m)\left(\frac{p^2+3p}{(p+1)(p+2)}\right) \tag{24b}$$

$$C_{11} = \frac{h^3}{12(1-\upsilon^2)}\left(\frac{E_c + E_m}{2}\right) \tag{24c}$$

$$\tilde{D} = \frac{J_1 + J_2}{(1-\upsilon^2)} \tag{25}$$

Where:

$$J_1 = \frac{-h^3(E_c - E_m)^2(p^2+3p)^2}{32(E_c + E_m)(p+1)^2(p+2)^2} \tag{26a}$$

$$J_2 = \frac{h^3(E_c + E_m)}{24} \tag{26b}$$

3.5 Equilibrium and compatibility equations for FGM plate

Consider a small solid element with dimensions d_x,d_y *and* d_z for the FGM plate under general load as shown in Fig. 8.

When element is in equilibrium, resultant forces in x-direction must be zero

$$(N_x + \frac{\partial N_x}{\partial x}dx)dy + (N_{yx} + \frac{\partial N_{yx}}{\partial y}dy)dx - N_x dy - N_{xy}dx = 0$$

or

$$\frac{\partial N_x}{\partial x} + \frac{\partial N_{yx}}{\partial y} = 0 \tag{27a}$$

Similarly, the resultant forces in y-direction yields,

$$\frac{\partial N_{xy}}{\partial x} + \frac{\partial N_y}{\partial y} = 0 \tag{27b}$$

$$\frac{\partial^2 M_x}{\partial x^2} + 2\frac{\partial^2 M_{xy}}{\partial x \partial y} + \frac{\partial^2 M_y}{\partial y^2} = \left[N_x \frac{\partial^2 w}{\partial x^2} + 2N_{xy}\frac{\partial^2 w}{\partial x^2 \partial y^2} + N_y \frac{\partial^2 w}{\partial y^2} \right] \tag{27c}$$

If the FGM plate is subjected to only in-plane loading, Eq. (27c) can be solved in terms of the stress function *f(x,y)* which is defined by

$$N_x = \frac{\partial^2 f}{\partial y^2}, \quad N_y = \frac{\partial^2 f}{\partial x^2} \text{ and } N_{xy} = \frac{\partial^2 f}{\partial x \partial y} \tag{28}$$

Substituting Eq. (27c) in to Eq. (28) provides stability equation which includes two dependent unknowns (deformation, *w* and stress function *f*).

$$\tilde{D}\nabla^4 w - (\frac{\partial^2 f}{\partial y^2}\frac{\partial^2 w}{\partial x^2} + 2\frac{\partial^2 f}{\partial x \partial y}\frac{\partial^2 w}{\partial x \partial y} + \frac{\partial^2 f}{\partial x^2}\frac{\partial^2 w}{\partial y^2}) = 0 \tag{29}$$

To obtain the second equation, compatibility equation needs to be used. From kinematic compatibility Eq. (11), it can be seen that

$$\frac{\partial^2 \varepsilon_{xx}}{\partial y^2} + \frac{\partial^2 \varepsilon_{yy}}{\partial x^2} - \frac{\partial^2 \gamma_{xy}}{\partial x \partial y} = \left(\frac{\partial^2 w}{\partial x \partial y} \right)^2 - \frac{\partial^2 w}{\partial x^2}\frac{\partial^2 w}{\partial y^2} \tag{30}$$

Substituting Eq. (28) into Eq. (30) yields

$$\nabla^4 f - I_1 \left[\left(\frac{\partial^2 w}{\partial x \partial y} \right)^2 - \frac{\partial^2 w}{\partial x^2}\frac{\partial^2 w}{\partial y^2} \right] = 0 \tag{31}$$

Equations (29) and (31) form two equations for the variables *w* and *f* which are used to compute the critical buckling load of the FGM plate using the Galerkin method which are also expressed in (J. C. Ezeh et al. 2014, Abdolvahab 2016).

3.6 Stability analysis of FGM plate under uniaxial compression

Consider a rectangular functionally graded plate subjected to an in-plane loading in x direction with simply supported edge in all sides (SSSS)

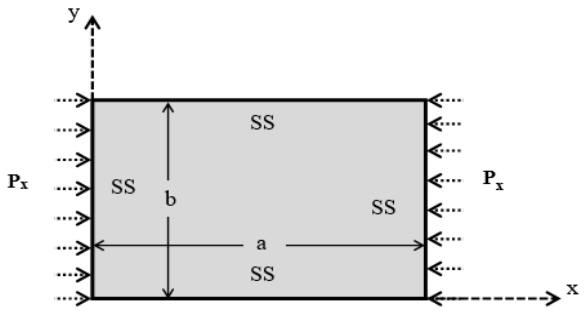

Figure 7: Rectangular FGM plate subjected to in-plane loading

Since the plate is considered simply supported along all edges, the boundary conditions are:

$$\begin{cases} w = 0 \\ M_x = 0 \end{cases} \quad at\ x = 0\ and\ x = a \qquad \begin{cases} w = 0 \\ M_y = 0 \end{cases} \quad at\ y = 0\ and\ y = b$$

The displacement field which satisfy the above boundary conditions can be selected as:

$$w = A_{\lambda_x \lambda_y} \frac{\sin \lambda_x \pi x}{a} \frac{\sin \lambda_y \pi y}{b} \qquad \lambda_x, \lambda_y = 1, 2, ... \tag{32}$$

Where λ_x and λ_y is number of half-waves in x- and y- directions respectively.
The Galerkin equation has the following form

$$\int_0^a \int_0^b \left[L\left(w_N\right) - p \right] f_i\left(x, y\right) dxdy = 0 \qquad i = 1, 2.. \tag{33}$$

Where

$$L\left(w_N\right) - p = \frac{\partial^4 w\left(x, y\right)}{\partial x^4} + 2\frac{\partial^4 w\left(x, y\right)}{\partial x^2 \partial y^2} + \frac{\partial^4 w\left(x, y\right)}{\partial y^4} + \frac{N_x}{\tilde{D}} \frac{\partial^2 w}{\partial x^2} + \frac{N_y}{\tilde{D}} \frac{\partial^2 w}{\partial y^2} \tag{34}$$

$$f_1(x, y) = \sin\frac{\pi x}{a} \sin\frac{\pi y}{b} \qquad f_2(x, y) = \sin\frac{2\pi x}{a} \sin\frac{2\pi y}{b}$$

Since there are two terms in the assumed displacement function, two Galerkin equations must be written and solving the differential equilibrium and compatibility using the Galerkin method, the FGM plate critical uniaxial buckling load is obtained as shown in Eq. 35. This result is same as from Shariat et al. (2005).

$$P_x = \frac{-\pi^2 \tilde{D}}{b} \frac{\left[\left(\frac{\lambda_x b}{a} \right)^2 + \lambda_y{}^2 \right]^2}{\left(\frac{\lambda_x b}{a} \right)^2} \tag{35}$$

4. Numerical buckling analysis of FGM plate

Numerical simulation for FGM plate buckling is performed using FE package ABAQUS for the three material functions. The plate was assumed to have same width (b=40 inch), aspect ratio of (a/b) 0.5 to 4.0 and plate thicknesses from 0.5 to 4.0 inches were considered. Modeling of the FGM plate is performed by considering ten layers across the plate thickness, each layer was

assumed to have isotropic and homogenous material property using the volume fraction and the overall thickness would attain a gradual variation of material property from one face to other. The Young's modules for metal (E_m) and ceramic (E_c) considered are 29500 ksi and 55114 ksi for metal and ceramic respectively. The poison ratio was assumed to be constant for each layer with a value of 0.3.

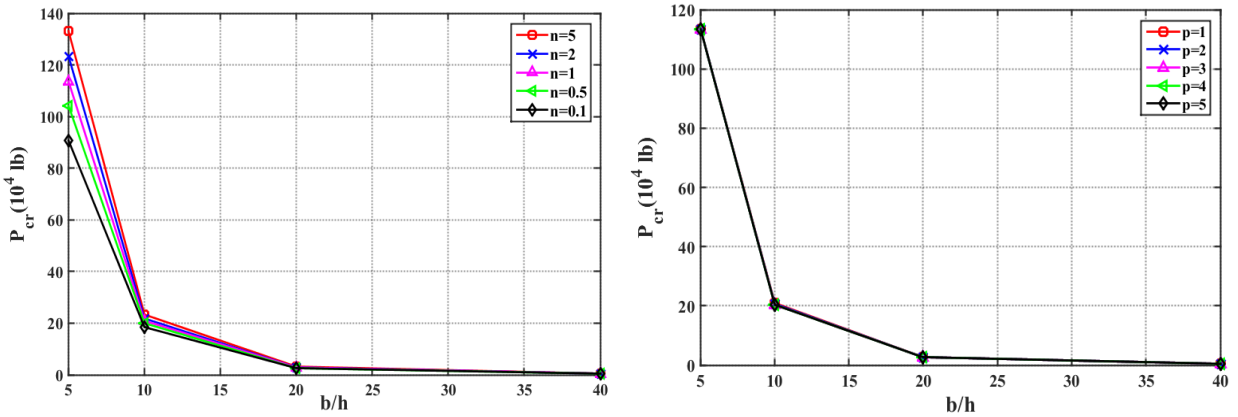

(a) (b)

Figure 8: Critical buckling load for a/b=4 (a) P-FGM and (b) S-FGM

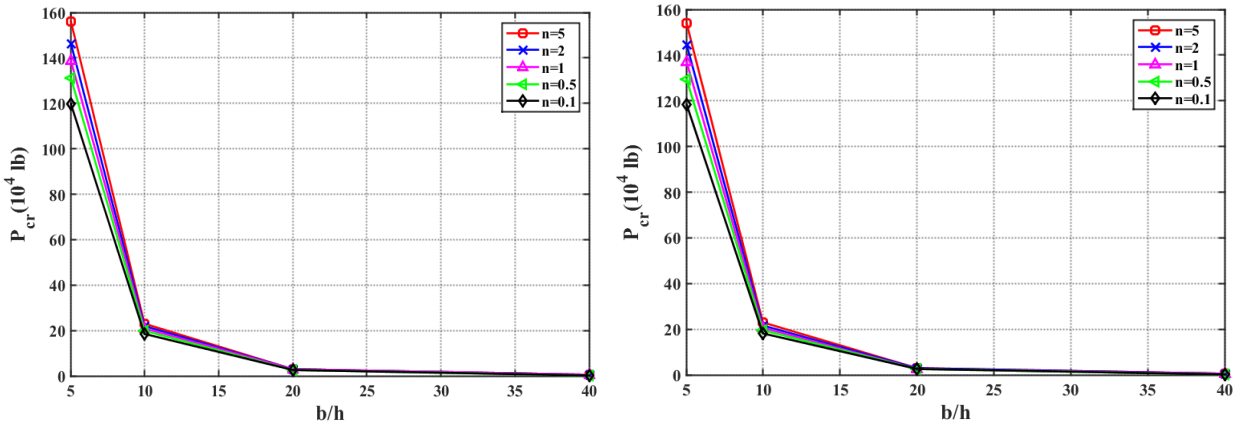

(a) (b)

Figure 9: Critical buckling load for P-FGM (a) a/b=3 and (b) a/b=2

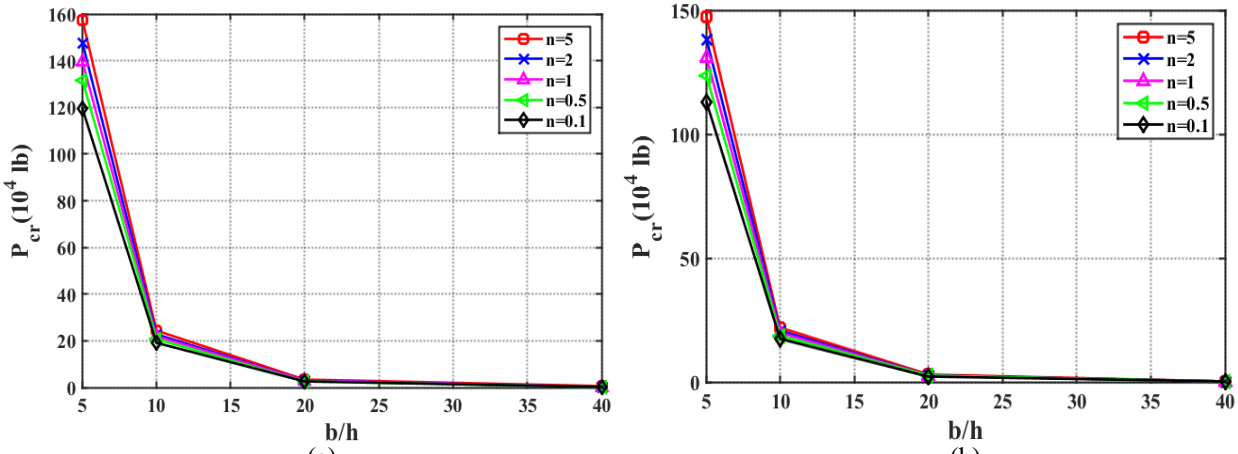

(a) (b)

Figure 10: Critical buckling load for P-FGM (a) a/b=1.5 and (b) a/b=1.0

From Fig. 6-10 it can be observed that the higher the FGM plate thickness the higher the critical buckling load in all the three FGM material functions. Another observation is that the Sigmoid function (S-model) results in relatively similar critical buckling loads for each plate thickness with varying p values. Exponential function (E-model) resulted in the smallest critical buckling loads in all aspect ratios considered in the analyses. Power-law function (P-model) with index n=5.0 resulted the highest critical buckling load not only among other n-values but also from all the three material functions considered. The first critical buckling mode has also been changed from a single half-wave for plate aspect ratio of 0.5 and 1.0 to four half-waves for aspect ratio of 4.0 and two and three half-waves in between. Critical buckling load shows three distinct patterns in P-FGM model, where there is a reduction in buckling load from aspect ratio 0.5 to 1.0 and increases from 1.0 to 1.5 and then decreases from 1.5-4.0.

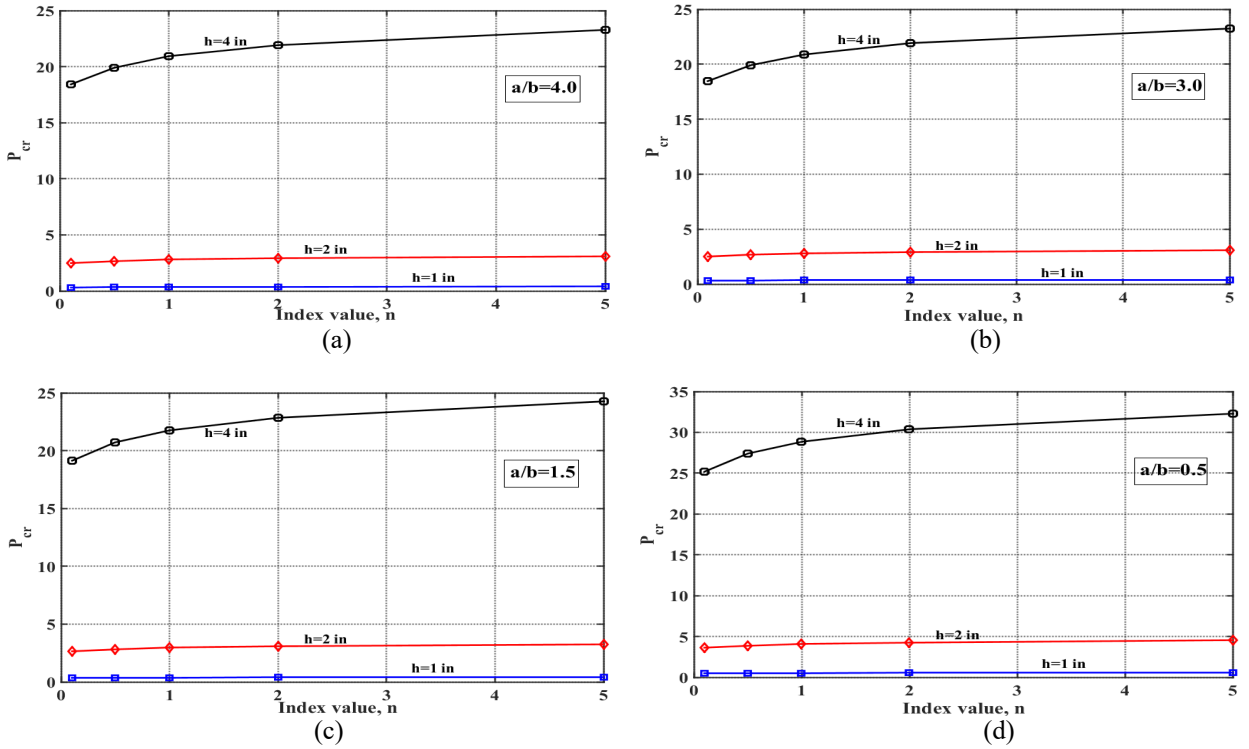

Figure 11: Critical buckling load versus index value for P-FGM model

Critical buckling load comparison for SSSS and CCCC boundary conditions for plate aspect ratio of 1.0 is presented in Tables 1 and 2 below. It can be observed that the critical buckling loads for fixed-fixed boundary condition for all power-law index values is higher than the one with simply supported FGM plate.

Table 1: Critical buckling load for SSSS FGM plate (10^4 lb) P-FGM model

h	b/h	n=5	n=2	n=1	n=0.5	n=0.1
8	5	147.22	138.336	130.948	123.688	112.960
4	10	21.999	20.740	19.774	18.828	17.4004
2	20	2.954	2.7884	2.666	2.5472	2.3658
1	40	0.3804	0.3592	0.3439	0.3289	0.3061
0.5	80	0.04818	0.0455	0.0436	0.04172	0.03885

Table 2: Critical buckling load for CCCC FGM plate (10^4 lb) P-FGM model

h	b/h	n=5	n=2	n=1	n=0.5	n=0.1
8	5	208.868	195.06	182.88	171.132	156.19
4	10	35.338	33.259	31.616	30.009	27.607
2	20	4.8848	4.609	4.4056	4.207	3.905
1	40	0.6292	0.5942	0.5689	0.5443	0.5066
0.5	80	0.0793	0.0749	0.0718	0.0687	0.0641

5. Conclusions

In this paper buckling analysis of a rectangular functionally graded plate was investigated through both analytical solution and numerical simulations. Analytical solution was obtained using the Galerkin method of solving differential equations which are derived from equilibrium and compatibility equations. Numerical simulation was also performed for all FGM material functions, aspect ratio and different boundary conditions. From the results, it was observed that the power-law function (P-FGM) with index n=5.0 resulted the highest critical buckling load for all plate aspect ratio and both plate boundary conditions. Sigmoid function (S-FGM) results in relatively similar critical buckling loads for each plate thickness and exponential function (E-FGM) resulted in the smallest critical buckling loads in all aspect ratios considered in the analyses. Critical buckling load for CCCC boundary conditions was observed to be higher than SSSS plate for all material functions, plate thickness as well as plate aspect ratio.

The results presented herein considered only uniaxial compression load, two boundary conditions. In order to fully understand the buckling behavior of FGM plates and to consider this newly developed materials for civil engineering application, future research effort need to extend these observations by conducting experimental tests, simplify the analytical solution for easy use and perform parametric study to include different loading conditions, boundary conditions and material models.

References

Abdolvahab, V. (2016). "Local Buckling of FGM Stiffened plates Subjected to Uniform Compression Using the Galerkin Method." Computations and Materials in Civil Engineering **1**(2): 85-97.

Abdolvahab, V. (2016). "Local Buckling of FGM Stiffened plates Subjected to Uniform Compression Using the Galerkin Method." Computations and Materials in Civil Engineering **Volume 1,** (No. 2,): 85-97.

Anil Gite, K. S. D. K. (2015). Stability Analyis of FGM Plate under In-Plane Compressive load. Proceedings of 60th Congress of ISTAM, Rajasthan, India.

Bever, M. S. a. M. B. (1972). "Gradients in polymeric materials." Journal of Materials Science(7): 741-746.

Bhavar, V., P. Kattire, S. Thakare, S. patil and R. K. P. Singh (2017). "A Review on Functionally Gradient Materials (FGMs) and Their Applications." IOP Conference Series: Materials Science and Engineering **229**.

Birman, V. and L. W. Byrd (2007). "Modeling and Analysis of Functionally Graded Materials and Structures." Applied Mechanics Reviews **60**(5).

Bodaghi, M. and A. R. Saidi (2010). "Stability analysis of functionally graded rectangular plates under nonlinearly varying in-plane loading resting on elastic foundation." Archive of Applied Mechanics **81**(6): 765-780.

Bohidar, S. K., R. Sharma and P. R. Mishra (2014). "Functionally Graded Materials: A Critical Review." International Journal of Research **1**(7): 2348-6848.

Chi, S.-H. and Y.-L. Chung (2006). "Mechanical behavior of functionally graded material plates under transverse load—Part I: Analysis." International Journal of Solids and Structures **43**(13): 3657-3674.

Ferreira, A. J. M., R. C. Batra, C. M. C. Roque, L. F. Qian and P. A. L. S. Martins (2005). "Static analysis of functionally graded plates using third-order shear deformation theory and a meshless method." Composite Structures **69**(4): 449-457.

J. C. Ezeh, M. O. Ibearugbulem, H. E. Opara and O. A. Oguaghamba (2014). "Galerkin's Indirect variational methos in Elastic Stability Analysis of Plates." International Journal of Research in Engineering and Technology **03**(04).

Karam Y. Maalawi, H. E. M. E.-S. (2011). "Stability Optimization of Functionally Graded Pipes Conveying Fluid." International Journal of Mechanical, Aerospace, Industrial, Mechatronic and Manufacturing Engineering **Vol:5, No:7**.

Kieback, B., A. Neubrand and H. Riedel (2003). "Processing techniques for functionally graded materials." Materials Science and Engineering: A **362**(1-2): 81-106.

Najafizadeh, M. M. and M. R. Eslami (2002). "Buckling analysis of circular plates of functionally graded materials under uniform radial compression." International Journal of Mechanical Sciences **44**(12): 2479-2493.

Qian, L. F., R. C. Batra and L. M. Chen (2004). "Static and dynamic deformations of thick functionally graded elastic plates by using higher-order shear and normal deformable plate theory and meshless local Petrov–Galerkin method." Composites Part B: Engineering **35**(6-8): 685-697.

Rasheedat M. Mahamood, E. T. A. (2012). "Functionally Graded Material. An Overview." Proceedings of the World Congress on Engineering 2012 **Vol III WCE 2012,London, U.K**.

Reddy, J. N. (2000). "Analysis of functionally graded plates." International Journal for Numerical Methods in Engineering(47): 663-684.

Sahari, B. B., S. Chen, W. Zhang, Y. Hao, Q. Qin and R. Das (2016). "Stability and Bifurcation Analysis of Functionally Graded Materials Plate Under Different Loads and Boundary Conditions." MATEC Web of Conferences **82**: 01013.

Shariat, B. A. S., R. Javaheri and M. R. Eslami (2005). "Buckling of imperfect functionally graded plates under in-plane compressive loading." Thin-Walled Structures **43**(7): 1020-1036.

Y. Miyamoto, W.A. Kaysser, B.H. Rabin, A. Kawasaki and R. G. Ford (1999). Functionally Graded Materials: Design, Processing and Application, Springer Science+Business Media LLC.